Thin-Walled Structures 144 (2019) 106250

Contents lists available at ScienceDirect

Thin-Walled Structures

journal homepage: www.elsevier.com/locate/tws

Full length article

Buckling of imperfect cylinder-cone-cylinder transition under axial compression

M.S. Ismail[a,c], O. Ifayefunmi[b,*], S.H.S.M. Fadzullah[a]

[a] Fakulti Kejuruteraan Mekanikal, Universiti Teknikal Malaysia Melaka, 76100, Melaka, Malaysia
[b] Fakulti Teknologi Kejututeraan Mekanikal dan Pembuatan, Universiti Teknikal Malaysia Melaka, 76100, Melaka, Malaysia
[c] Bahagian Kompetensi dan Peningkatan Kerjaya, Jabatan Pendidikan Politeknik dan Kolej Komuniti, Putrajaya, 62100, Malaysia

ARTICLE INFO

Keywords:
Cylinder-cone-cylinder transition
Buckling
Eigenmode imperfection
SPLA imperfection
Axisymmetric outward bulge
Structural stability

ABSTRACT

This paper presents the numerical investigation results focusing on the buckling behavior of geometrically imperfect cylinder-cone-cylinder transition subjected to axial compression. The models are assumed to be made from unalloyed mild steel. Several initial geometric imperfections techniques such as (i) Eigenmode imperfection approach, (ii) Axisymmetric outward bulge and (iii) Single Perturbation Load Analysis (SPLA) imperfections were superimposed on the perfect cylinder-cone-cylinder shell. Reduction of the buckling strength was then quantified numerically. As expected, the buckling strength of cylinder-cone-cylinder shells was strongly affected by initial geometric imperfection and the reduction in buckling strength was seen to be strongly dependent on the approach and the location of imperfection. Eigenmode imperfection is seen to produce the lowest knock-down factor, followed by axisymmetric outward bulge and SPLA imperfections, respectively. Finally, the lower bound knockdown factors that can be implemented for design purposes has been proposed for the worst initial geometric imperfection case, i.e., Eigenmode, imperfections.

1. Introduction

Thin-walled shells such as cylinder, cone or combination of both are widely used in many industrial applications. When in use, these shells are often exposed to various type of loading which includes external pressure, internal pressure, axial compression, bending, torsion etc., or combination of each load. The shells wall thickness are mostly designed according to their industrial application. For example, thinner shells are extensively used in aeronautic/aerospace industry. Thus, their failure is limited by elastic buckling. While thicker shells are predominantly used in marine and offshore industries where the mode of failure is largely due to plastic buckling. Under various loading conditions, the state of stress in the multi-segment shell of revolution assembly is predominantly membrane stress away from the intersection, but as the intersection is being approached from either the top or the bottom, the state of stress in the shell will change from membrane stress to a combination of membrane stress and bending stress [1–5]. In general, the failure of cone-cylinder assembly mostly occurs at the intersection. This behavior can be attributed to the slope discontinuity in the shell meridian at the intersection, thereby resulting in local bending and circumferential stresses at the junction [1]. As a result of the local weakening effect at the intersection, reinforcement is often used to strengthen the shell at the junction either by increasing the thickness of the shell at the junction or by introducing a ring at the intersection [1]. Zingoni [1] developed an equation to quantify the discontinuity effects at the junction of cone-cone assembly for arbitrary loading. In the equation, the membrane solution for the shell was taken as the particular integral of the bending equation. Furthermore, discontinuity effect was obtained by imposing conditions of geometric continuity and equilibrium at the shell junction.

It is a general believe that thin-walled structures subjected to various loading conditions are prone to imperfection. In addition, the uncertainties are unavoidable for real-world thin-walled structures, which may cause great influence on the practical load-carrying capacity [6]. Moreover, the influence of initial geometric imperfection on the buckling behavior of combined cone-cylinder assembly is still a puzzling issue for engineer/designer as it may possibly reduce the buckling strength of the shell structures. Questions on how it has been defined, positioned, maximum amplitude, worst shape etc. allow the designer to prepare for the worst case scenario (e.g., unexpected catastrophic structural failure [7]). Since most cone-cylinder transition assembly in practice is susceptible to initial geometric imperfection, the buckling behavior of imperfect cone-cylinder transition would be beneficial to the industries. A comprehensive review of the buckling behavior of

* Corresponding author.
E-mail address: olawale@utem.edu.my (O. Ifayefunmi).

https://doi.org/10.1016/j.tws.2019.106250
Received 27 November 2018; Received in revised form 3 June 2019; Accepted 12 June 2019

imperfection sensitivity of cone or cylinder under various loading conditions was reported in Ref. [6].

Eigenmode imperfection approach is a popular method that is widely used by many researchers to introduce structural imperfection. References [8–14] are devoted to cone, while Refs [15–19] cover Eigenmode imperfection of cylinder. The method uses the Eigenmode shapes with different weighting of imperfection amplitude. Ifayefunmi and Błachut [13,14] numerically analyzed the influence of Eigenmode imperfections on the buckling strength of truncated cones subjected to axial compression, lateral pressure, and combined axial compression and external pressure. The cones were assumed to be relatively thick, therefore failing in the elastic-plastic domain. The ratio of the amplitude of imperfection, w_o, to the cone wall thickness, t (i.e., w_o/t), was varied between 0.0 and 1.0. Ifayefunmi and Błachut [14] further examined initial geometric imperfection in the form of (i) axisymmetric outward bulge (for axial compression only), (ii) a "single wave" extracted from Eigenmode and a localized smooth dimple (for lateral pressure only) and (iii) combined axisymmetric outward bulge and a single wave extracted from Eigenmode (for combined loading). The influence of initial geometric imperfection sensitivity on cone subjected to combined axial load and lateral pressure, within the elastic-plastic regime was numerically analyzed in Refs. [20,21]. In practice, most imperfections found in structures do not have such buckling modeshape. Eventually, the used modeshape would often be on trials to estimate the lowest buckling load.

The single perturbation load approach (SPLA) which was proposed by Hühne et al. [22] is relatively a new method to introduce initial geometric imperfection. The method uses the influence of a single lateral load applied to the surface of the model (e.g., mostly at midsection) to simulate the worst geometrical imperfection of typical structure. The applied lateral load will produce a local-dimple that acts as the imperfection. At this local-dimple, buckling will begin which will then trigger instabilities (i.e., local and global) to the structure. Several researchers [15,16,23] suggest that Single Perturbation Load Analysis (SPLA) imperfection approach is less conservative in estimating the buckling load. There have been several investigations on the initial geometric imperfection sensitivity of (i) cones [24,25] and (ii) cylinders [8,17,26–28] by adopting the SPLA method. Nonetheless, a correlation between Eigenmode imperfection and SPLA imperfection techniques were reported in Refs. [15,29] with many positive reviews towards the latter.`

In Refs. [30,31], multiple lateral loads along the cylinder circumference were suggested to demonstrate the worst kind of imperfection level. The test was carried out to describe the range of worst `multiple perturbation load approach (WMPLA). As a result, the MPLA gives more conservative results than the SPLA and in some extreme cases, leads the knockdown factor closer to NASA SP 8007 guideline [32]. In addition, some newly develop methods are (i) Single Boundary Perturbation Approach (SBPA) [27,33] and (ii) Single Perturbation Displacement Approach (SPDA) [27].

To-date, there is no new information on the imperfection sensitivity of cylinder-cone-cylinder transition subjected to axial compression since the work by Dinkler and Knoke [34]. Therefore, this paper aims to provide relevant insight into the influence of imperfection amplitude on the buckling behavior of axially compressed cylinder-cone-cylinder transition. Three (3) types of imperfection techniques were considered namely; (a) Eigenmode imperfection, (b) Axisymmetric outward bulge and (b) Single Perturbation Load Analysis (SPLA). For SPLA imperfection, first, the lateral perturbation load is applied at (i) top cylinder mid-section, (ii) cone mid-section and (iii) bottom cylinder mid-section. Then, the lateral load is applied along the cone slant length to further analyze the imperfection sensitivity of cylinder-cone-cylinder. The present work is entirely numerical using ABAQUS finite element (FE) code and it validates the experimental results reported in Ref. [35], for perfect unstiffened cylinder-cone-cylinder assembly. Therefore, the content of the paper will concentrate and be limited to imperfection sensitivity of unstiffened cylinder-cone-cylinder transition subjected to axial compression.

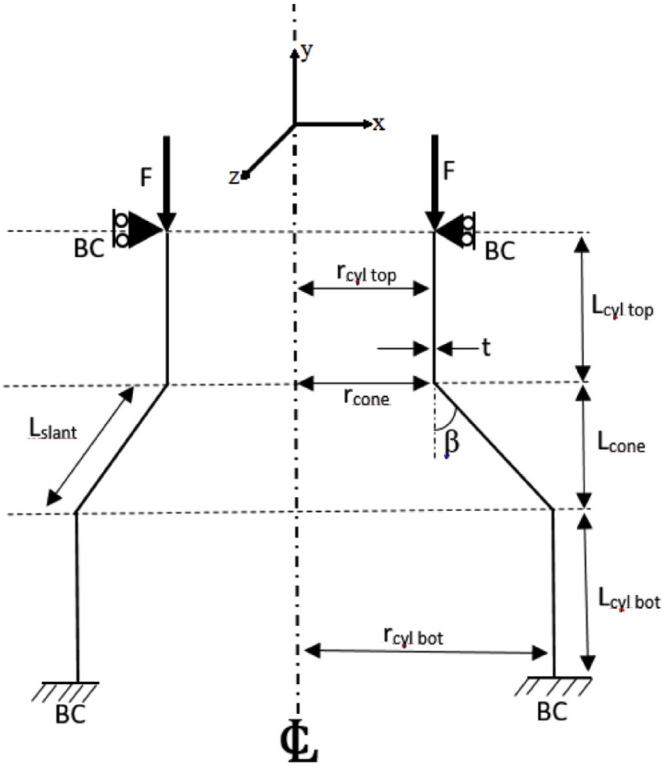

Fig. 1. Geometry of cylinder-cone-cylinder transition subjected to axial compression.

2. Numerical modeling

A configuration of combined cylinder and cone shells subjected to axial compression was considered in the analysis. The combined shell configuration is made from two (2) different size of cylinders (i.e., $r_{cyl\ top}$ and $r_{cyl\ bot}$), with a cone (r_{cone}) as transition medium in between the two cylinders. The shell consists of slant length of the cone, L_{slant}, length of two (2) different cylinders, (i.e. $L_{cyl\ top}$ and $L_{cyl\ bot}$) and cone angle, β, as illustrated in Fig. 1. Two (2) different shell thickness were considered in the study (i.e. t = 0.5 mm and t = 1 mm). The shell is assumed to have a uniform wall thickness. Constant cone angle was considered, i.e., $\beta = 20^{\circ}$. The shell geometric parameters are given in Table 1. Specimens were presumed to be made from mild unalloyed steel Stl 2 (Material-No. 1.0330) with material properties given in Table 2.

First, preliminary numerical calculations were carried out to benchmark the experimental data presented in ECCS [35] part C for perfect cylinder-cone-cylinder shells (ZKZ-XV50 and ZKZ-XV10 models). This seems necessary to confirm the appropriateness of the numerical approach adopted in this paper. Non-linear static analysis was carried out using the modified Riks method algorithm which is implemented in ABAQUS. The algorithm is based on Lagrangean formulation for moderately large deflections. The finite element analysis was carried out using axisymmetric shell element (SAX2 in ABAQUS element library) and four-node shell element with six degrees of freedom (S4R in ABAQUS element library). Five integration points across the shell wall were used to estimate the spread of plastic strain along the shell wall. Table 3 present the result of the convergence study of the FE models. The result shows that 24192 elements are sufficient for the analysis. Under axial compression, the boundary conditions applied to the bottom end of the assembly are $u_x = u_y = u_z = \phi_x = \phi_y = \phi_z = 0$. The same boundary condition was

Table 1
Geometrical properties of analyzed models in referring to Ref. [30].

Model no.	$r_{cyl\ top}$	$r_{cyl\ bot}$	r_{cone}	$L_{cyl\ top}$	$L_{cyl\ bot}$	L_{cone}	t	β (○)	$r_{cyl\ bot}/t$
	(mm)								
ZKZ-XV50	152	225	152	300	500	200	0.5	20	450
ZKZ-XV10	152	225	152	300	500	200	1	20	225

Table 2
Material properties used in the analysis in referring to Ref. [30].

Model no.	E [GPa]	σ_{Yield} [MPa]	υ
ZKZ-XV50	211	225	0.3
ZKZ-XV10	201	206	0.3

Table 3
Results of the mesh sensitivity for the benchmarked models.

No. of element	ZKZ-XV50	ZKZ-XV10
	F_{coll} [kN]	
5226	38.793	89.773
11817	34.113	82.841
18688	32.244	79.617
24192	31.339	78.134

applied at the top end of the assembly except for $u_y \neq 0$. Furthermore, at the cylinder-cone junction, the equation of continuity of displacement is given by: $u_{x(cyl)} = \bar{u}_{x(con)}$; $u_{y(cyl)} = \bar{u}_{y(con)}$ and $u_{z(cyl)} = u_{z(con)}$. The notation used above assumes: u ≡ displacements (u_x, u_y, u_z are local coordinate and $\bar{u}_x$, $\bar{u}_y$ are global coordinate), and ϕ ≡ rotations. In the finite element calculations, the material is modeled as elastic perfectly plastic using J2 flow plasticity theory. Although, it has been found that the flow theory gives higher buckling loads than deformation theory but the difference is appreciable only at low values of the power exponents [36,37]. However, numerical calculation for cylinder-cone-cylinder shells (ZKZ-XV50) shows that the J2 flow plasticity theory is sufficient.

Validation of experimental results for all models (i.e., ZKZ-XV50 and ZKZ-XV10) with their corresponding buckling loads are given in Table 4. The ratio of experimental to numerical buckling load for model ZKZ-XV50 and ZKZ-XV10 are 0.996 and 1.244 respectively. Evidently, the predicted buckling load by ZKZ-XV10 model recorded a reasonable discrepancy against the experiment results by nearly 20%. Nonetheless, the recorded discrepancy of ZKZ-XV10 model is expected, as the issue was previously addressed by means of having six (6) independent study to further benchmark the tested model. In addition, the given six (6) independent results are in agreement with the current numerical result within differences of 1.5%–6.5% as reported in Ref. [35]. Therefore, it can be suggested that the numerical model is appropriate for this analysis.

Table 4
Comparison of experimental and numerical results for the axially compressed cylinder-cone-cylinder transition. The number in parenthesis is F_{extpl}/F_{coll}.

Model no.	F_{exptl}	ECCS [30]	F_{num}
	[kN]		
ZKZ-XV50	31.2	54.401 (0.574)	31.339 (0.996)
ZKZ-XV10	97.2	153.801 (0.632)	78.134 (1.244)

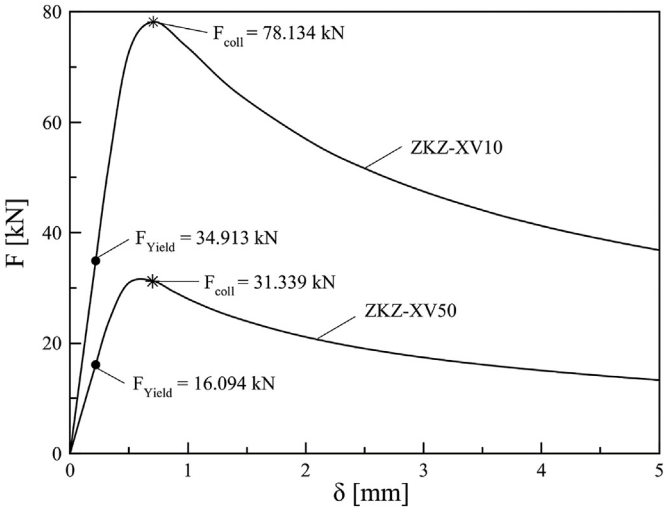

Fig. 2. Plot of load versus deflection of axially compressed cylinder-cone-cylinder intersections for perfect model.

2.1. Failure mechanism of cylinder-cone-cylinder

A typical plot of axially compressed cylinder-cone-cylinder models against axial shortening is shown in Fig. 2, indicating the first yield load, F_{Yield} and collapse load, F_{Coll}. It is apparent that the cylinder-cone-cylinder transitions reached their first yield load, F_{Yield}, at 16.094 kN and 34.913 kN for ZKZ-XV50 and ZKZ-XV10 models. The collapse loads, F_{Coll} were found to be 31.339 kN and 78.134 kN for both models. It can be seen that as the shell thickness increases, the load carrying capacity of the cylinder-cone-cylinder transition also increases accordingly. This agrees very well with available design codes which suggest that shell's buckling load are highly dependent on their thickness [32,35]. From Fig. 2, it can be seen that the plotted buckling load is nearly linear up to yield and collapse loads. A smooth drop of buckling load is observed once the collapse load is reached, in which a similar trend is observed for both models. The analysis also indicates that the buckling behavior of the cylinder-cone-cylinder is controlled by plastic buckling – the elastic analysis predicts higher buckling load than the elastic-plastic analysis as exemplified for perfect cylinder-cone-cylinder model ZKZ-XV50 in Fig. 3.

The spread of plastic strain through the shell wall thickness at yield and collapse for both models is illustrated in Fig. 4. The spread of plastic strain was observed to begin from the outer surface at both intersections and further continue to grow through the wall thickness. As expected, this can be attributed to membrane stress discontinuity at the intersection, reflecting the localized and rapidly changing behavior of bending disturbances [1]. As the magnitude of the axial force increases, the plastic strains progressively extend through the wall thickness of the shell and along the intersection length. Evidently, the results demonstrated that the smaller the radius-to-thickness ratio (r/t), the higher the spread of plastic strain in the shell. Similar to those reported in the past literature [38,39], the largest plastic strain was noticed to appear at the outer surface of the cylinder-cone-cylinder's top intersection. The bending-disturbance stresses at the top intersection is believed to be greater than those at the lower intersection because the larger axial

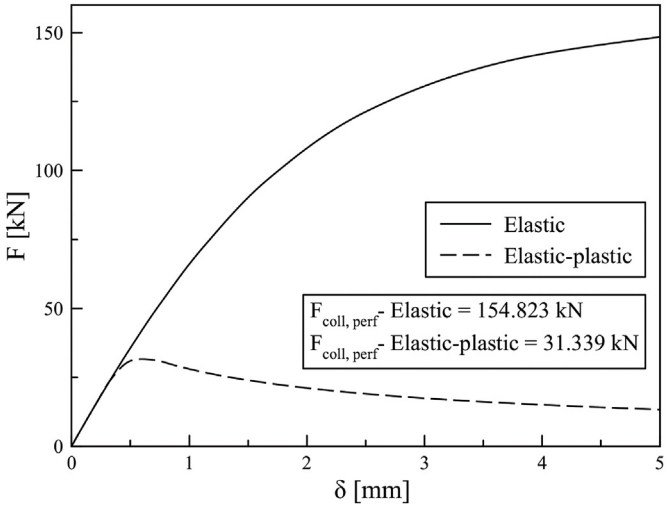

Fig. 3. Plot of elastic and elastic-plastic load versus deflection of axially compressed cylinder-cone-cylinder intersections for perfect model ZKZ-XV50.

compression in the top intersection results in larger membrane deformation incompatibilities, thereby inducing larger bending stresses at the top junction [2]. It is worth noting here that the spread of plasticity for both structures agreed well with the buckling modeshape produced by bifurcation analysis (see Fig. 5 (a)). The entire structure failed due to material plasticity instead of structural stability as suggested by Ref. [34].

3. Imperfect cylinder-cone-cylinder transition – Eigenmode shape, axisymmetric inward/outward bulged and SPLA imperfection

It is widely accepted that most thin-walled structures are affected by the presence of initial geometric imperfections. The presence of initial geometric imperfection is inevitable due to the manufacturing process or accidental damage [34]. Normally, knockdown factors are used to estimate the structural load carrying capacity under the influence of initial geometric imperfection. The knockdown factor is define as a normalized magnitude between the imperfect and perfect shell loads (i.e. F_{imp}/F_{Coll}). The knockdown factors are derived from the known worst case scenario the shells may experience (Eigenmode imperfections, SPLA, MPLA, GNA, etc.). To examine the influence of initial geometric imperfection on shells buckling strength of cylinder-cone-cylinder transition, three (3) types of imperfections were considered using ABAQUS finite element analysis namely; (i) Eigenmode (Fig. 5 (a)), (ii) SPLA imperfection at cone midsection (Fig. 5 (b)), bottom cylinder midsection Fig. 5 (c)), top cylinder midsection Fig. 5 (d)) and (iii) Axisymmetric outward bulged (Fig. 5 (e)). These imperfections were distinctly superimposed on the perfect model and the range of imperfection amplitude, w_o, were investigated. The imperfection amplitude to wall thickness ratio, w_o/t, was varied between 0 and 4. The following sub-section provides a detailed study on the effect of Eigenmode, Axisymmetric outward bulge and SPLA imperfections on the buckling load of cylinder-cone-cylinder transition. It must be noted that only ZKZ-XV50 model was analyzed for the imperfection study due to its close agreement of buckling load between the experimental and current numerical results.

3.1. Eigenmode shape imperfection and axisymmetric outward bulged

This section examines geometrically imperfect (i.e. eigenmode) cylinder-cone-cylinder transition subjected to axial compression. In the numerical calculation, four-noded shell element with six (6) degrees of freedom (S4R) was used. In order to obtain the Eigenmodes, eigenvalue buckling procedure using subspace solver was carried out first. A

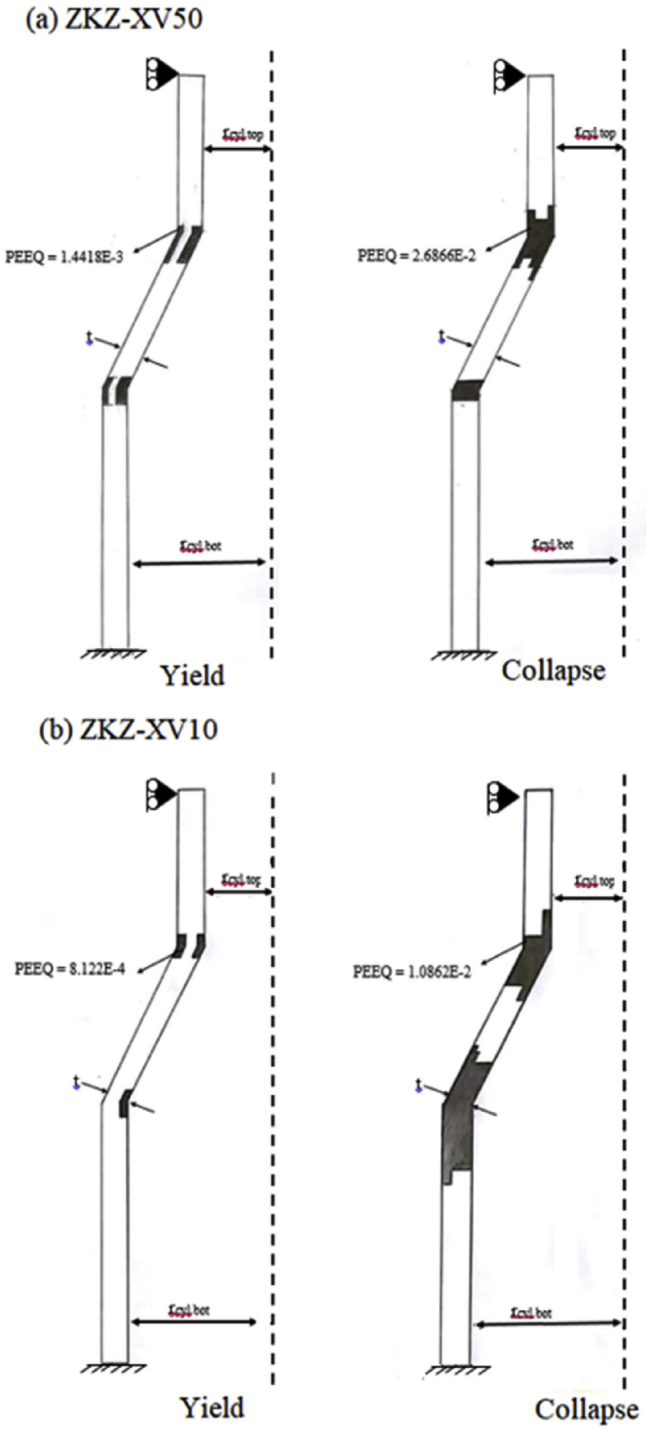

Fig. 4. Spread of plastic strain at yield and collapse for cylinder-cone-cylinder transitions under axial compression.

number of Eigenmodes were considered in the finite element analysis and the effect of them being superimposed with different range of imperfection magnitude. The range of imperfection amplitude considered for the analysis are chosen to be $0 < w_o/t < 4$. The modes were varied between n = 1 and 7, as shown in Fig. 6. The reason for using several Eigenmodes shape is necessary in order to estimate the shell's lowest knockdown factor. In this study, the selection of tested mode shapes was based on their worst buckling mode appearance. Following this, a non-linear static analysis using modified Riks method were carried out to obtain the collapse buckling load of axially compressed cylinder-cone-cylinder transition. The use of non-linear static Riks method to

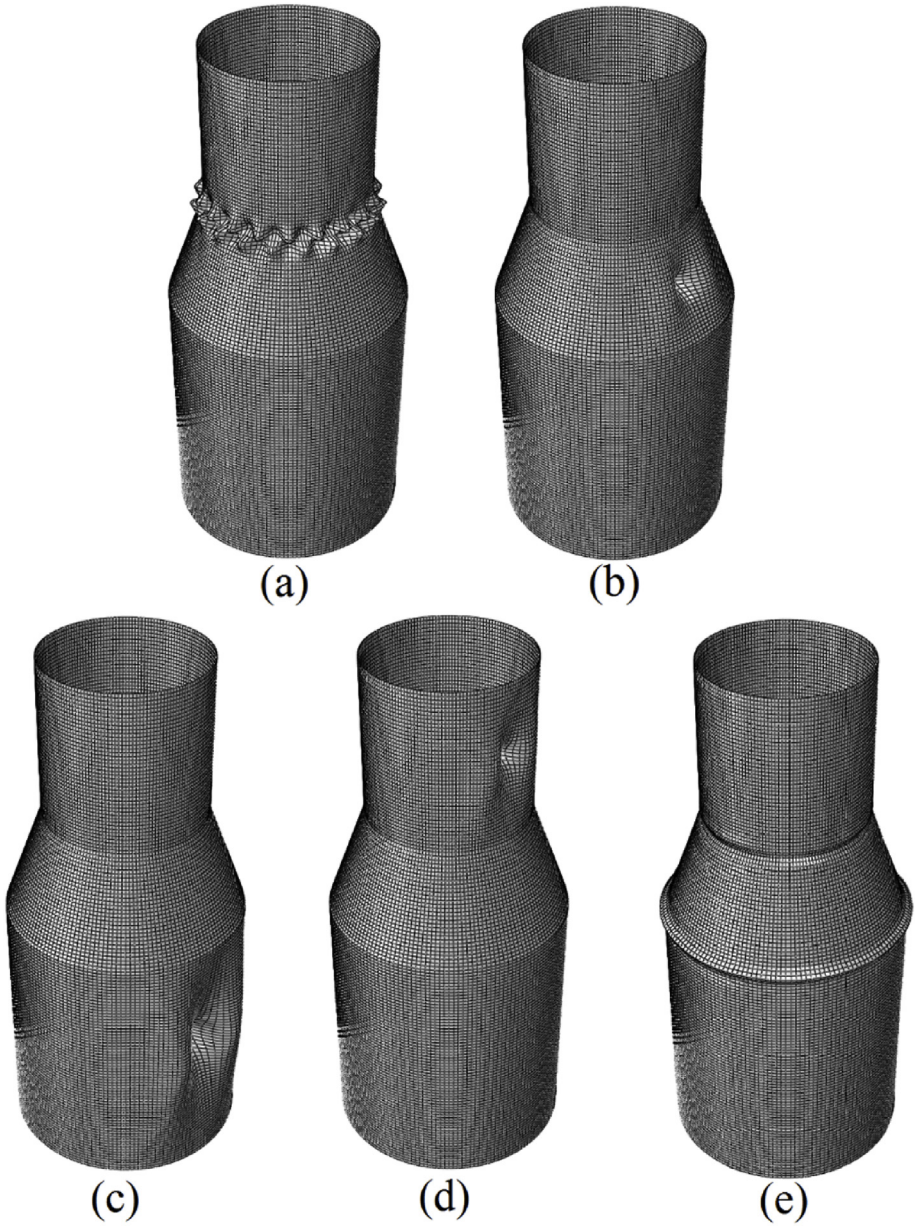

Fig. 5. Illustration of imperfection shape for (a) Eigenmode, (b) SPLA-cone midsection, (c) SPLA bottom cylinder midsection, (d) SPLA-top cylinder midsection and (e) Axisymmetric outward bulged.

compute the magnitude of the collapse load of the cylinder-cone-cylinder transition is appropriate – since there was no bifurcation between zeros to the collapse load (Riks method) as shown in Fig. 3.

Fig. 7 illustrates the effect of Eigenmode imperfection amplitude on the buckling strength of the cylinder-cone-cylinder model using Riks method. From the given results, it can be seen that mode shape, n = 5 produced the lowest knockdown factor. From the analysis, it is evident that the first mode shape may not serve as the worst-case geometrical imperfection and its consistent with references [17,29]. The estimated knockdown factor is recorded to be 0.789 at $w_o/t = 2$ for Eigenmode approach. Furthermore, the cylinder-cone-cylinder transition can only support about 79% of the load carrying capacity of the perfect shell with the presence of Eigenmode imperfection that is twice of the shell's thickness (i.e., $w_o/t = 2$). Beyond this imperfection amplitude, the effect of Eigenmode imperfection on the buckling strength of the shell is steadily depleting. For example, at $w_o/t = 4$, the cylinder-cone-cylinder transition can only withstand approximately 68%, of the load carrying capacity of the perfect shell. The obtained results clearly demonstrated that Eigenmode imperfection approach is capable of estimating the lower-bound knockdown factor but greatly reliant on the selected mode shape and the imperfection amplitude.

Fig. 8 shows the effect of Axisymmetric outward bulge with varied imperfection amplitude on the buckling strength of cylinder-cone-cylinder. A comparison was made between worst Eigenmode imperfection approach and Axisymmetric outward bulge. The Axisymmetric outward bulge was executed by taking the perfect shell's buckling deformation from the non-linear static Riks analysis to be the imperfection shape. Once suitable buckling deformation is found, which in this case, at 22nd increment (i.e., peak load), the shape is retained and varied with given imperfection amplitude in the subsequent analysis. As compare to Eigenmode imperfection, a similar trend was observed, the plotted curve of knockdown factors against imperfection amplitudes steadily reduced in the range of $0 < w_o/t < 4$. At $w_o/t = 2$, the cylinder-cone-cylinder transition reduces its load carrying capacity of the perfect shell by 10%, and further decreases by 19% at $w_o/t = 4$. It is worth noting that a conservative knockdown factor was estimated by Eigenmode

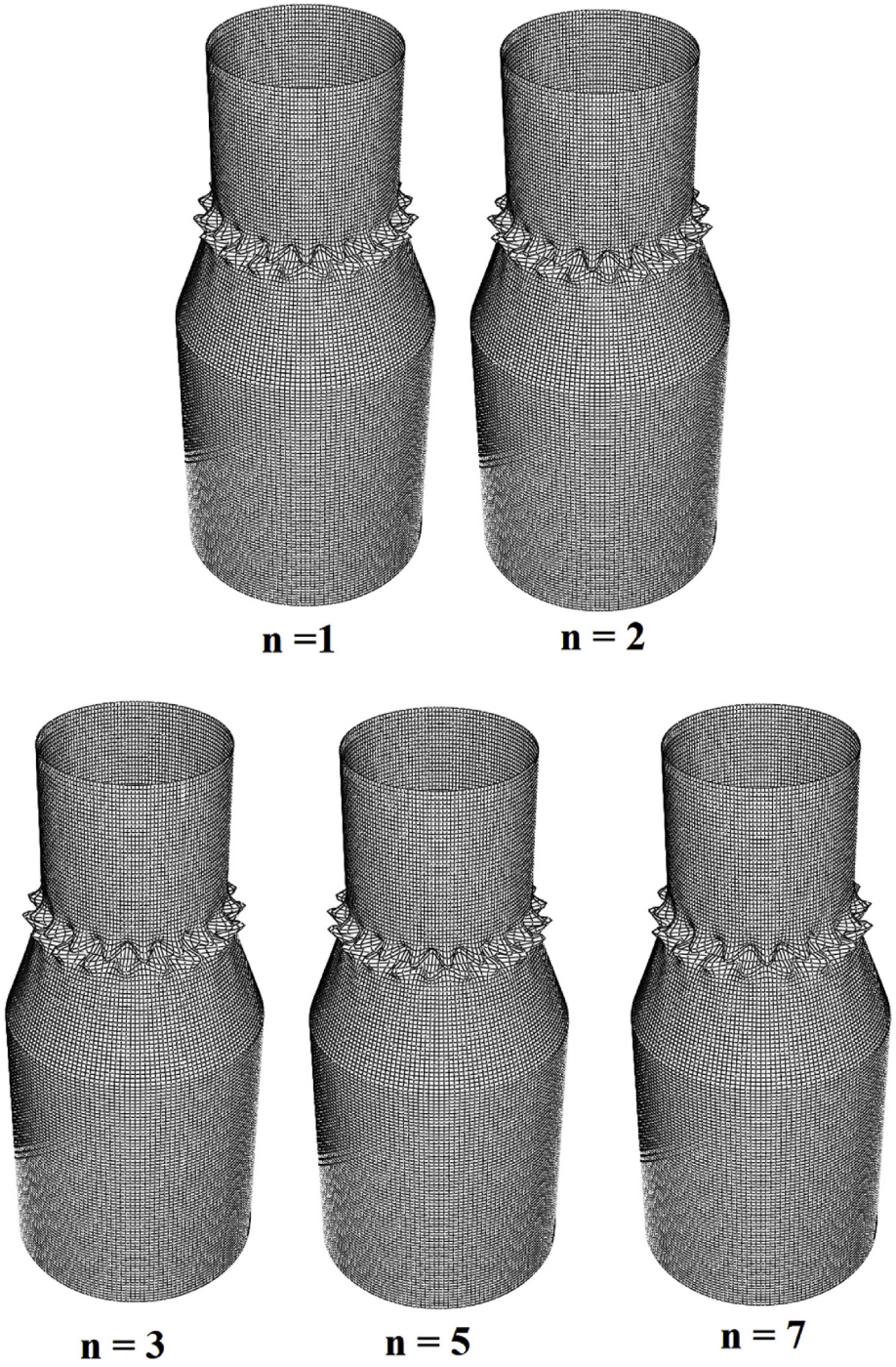

Fig. 6. Buckling mode shapes, n = 1, …, 7, for cylinder-cone-cylinder transition subjected to axial compression.

imperfection approach in comparison to Axisymmetric outward bulge. Fig. 9 on the other hand, shows the load-deflection curve for point marked 'A' and 'B' (i.e., $w_o/t = 2$) in Fig. 8. This may not be generally true for all material behavior. Depending on the material behavior of the structures (i.e., elastic behavior and/or elastic-plastic behavior), the response to imperfection is very different. Hence, the predicted knockdown factor will be different as shown in the load versus deflection curve for cylinder-cone-cylinder structure with eigenmode imperfection (n = 5 and $w_o/t = 2$) for elastic behavior (Fig. 10) and elastic-plastic behavior (Fig. 11). Here the cylinder-cone-cylinder structure with elastic material behavior predicts a knockdown factor of 0.62 as compared to the same structure having elastic-plastic material behavior with knockdown factor of 0.79.

3.2. Single pertubation load analysis (SPLA) imperfection

The SPLA imperfection approach was considered to be the worst, realistic and stimulating imperfection technique when considering the imperfection sensitivity of axially compressed cylinders [22]. The axially compressed cylinder-cone-cylinder transition is examined in this section. In general, as highlighted by Hühne et al. [22], the procedure of the SPLA in the finite element analysis has three steps. First, lateral perturbation load, $P_{Perturb}$ is applied at the mid-section of the shell. This is intended to produce a single buckle or a local dimple on the shell. The magnitude of lateral perturbation load, $P_{Perturb}$ is linearly increased until consistent buckling load is accomplished. Then, the shell is driven by axial compression until the buckling load is reached.

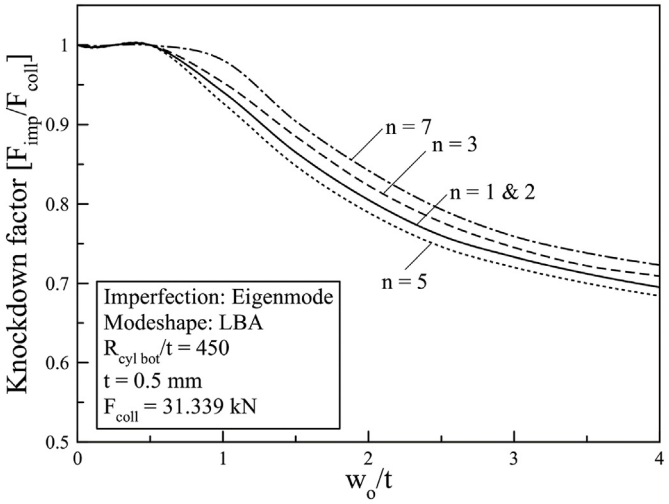

Fig. 7. Effect of imperfection amplitude and Eigenmode on the buckling strength of the cylinder-cone-cylinder transition.

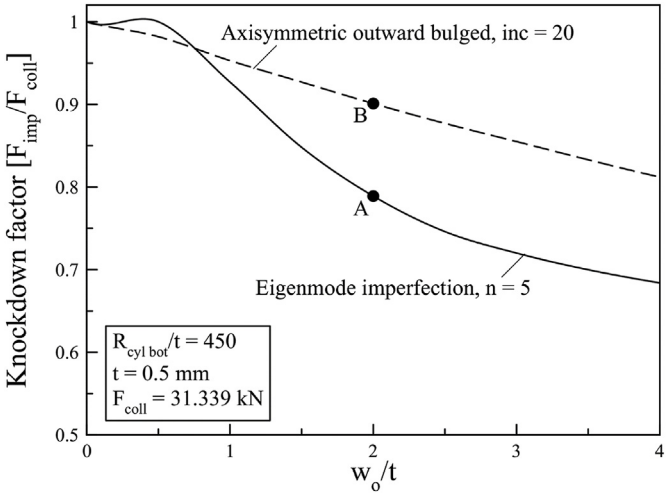

Fig. 8. Reduction of buckling strength as a function of imperfection amplitude, w_o/t. Comparison of imperfection amplitude between the worst imperfection approaches: Eigenmode Analysis and Axisymmetric outward bulged curves.

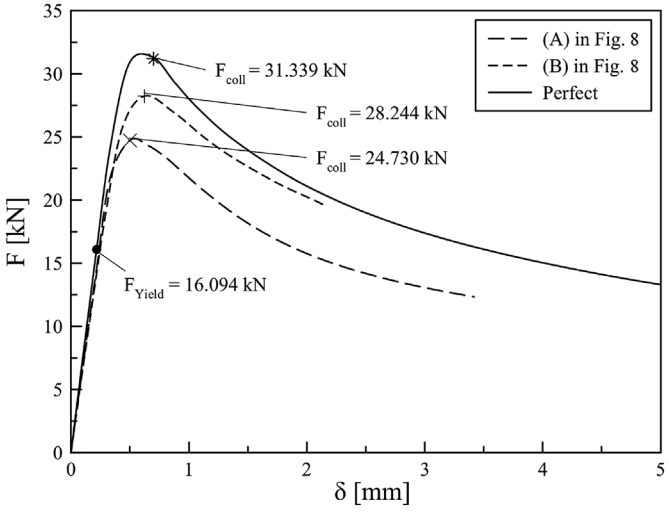

Fig. 9. Load-deflection curves for point (A) and (B) in Fig. 8 with perfect cylinder-cone-cylinder shell.

Fig. 5 (b) – (d) depict the SPLA imperfection shape considered in this section. The lateral perturbation load is applied at three different locations, they are: (i) cone midsection (Fig. 5 (b)), (ii) bottom cylinder mid-section (Fig. 5 (c)), and (iii) top cylinder midsection (Fig. 5 (d)). The analysis is then followed by executing the axial compression load until the shell reached collapse state. The bottom of the shell is fully clamped, during the application of lateral load in order to extract the worst possible deformation that might occur. Subjected to axial compression, the cylinder-cone-cylinder intersection's top end (cylinder section) is allowed to move in the axial direction while the other direction is fully clamped.

The sensitivity of buckling load to SPLA imperfections is depicted in Fig. 12 for cylinder-cone-cylinder transition under axial compression. From the given result, it is seen that buckling strength is not affected at all for dimples at both cylinder midsections. On the other hand, cone midsection appears to be more sensitive to imperfection amplitude from $1 < w_o/t < 4$. Apparently, at $w_o/t = 2$, the load carrying capability of shell drop by 3%. The buckling load further reduces to 13% once the magnitude of imperfection amplitude reached $w_o/t = 4$.

Since cone is more sensitive to shell buckling load, it was decided to further investigate the sensitivity of buckling load by applying the perturbation load along the cone slant length. Fig. 13 illustrates the location of the applied perturbation load along the cone slant length. The sensitivity of buckling load to SPLA imperfections along the cone slant length is depicted in Fig. 14 for cylinder-cone-cylinder transition under axial compression. From the given result, an identical curve was found by applying the SPLA at top and midsection of cone separately. Although the cone at midsection produced much lower buckling load than the later, as the SPLA moves towards the intersection between the lower cone and top big cylinder – the buckling strength starts to drop at smaller imperfection amplitude ($w_o/t < 2$). Conversely, beyond the range of imperfection amplitude of $2 < w_o/t < 4$, the plotted knockdown factors are marginally increased, and this is experienced by both analyses. A noticeable similarity of the situation was encountered in externally pressurized composite prolate ellipsoid reported in Ref. [40]. Nonetheless, the results explicitly showed that buckling load is more affected by applying the SPLA at cone low bottom in comparison to the other tested locations at $w_o/t \leq 2$. However, for $w_o/t > 2$, there is a transition in the region where the cylinder-cone-cylinder buckling load is more sensitive to SPLA imperfection. The knockdown factors, at $w_o/t = 4$, were found to be (i) SPLA – cone midsection (0.871), (ii) SPLA – cone top (0.953), (iii) SPLA – cone bottom (0.922) and (iv) SPLA – cone low bottom (0.912). The drop of shells buckling strength was computed to be in the range of 5%–13% at $w_o/t = 4$, in comparison to the perfect shell. The plot of load versus displacement for point 'C' in Fig. 14 indicates that the cylinder-cone-cylinder structure with SPLA imperfection exhibit a local buckling phenomena as shown in Fig. 15. This trend is consistent with that presented for composite conical structures in Ref. [25].

4. Comparison between Eigenmode shape, axisymmetric inward bulged and SPLA imperfection

A comparison of knockdown factor estimated by worst Eigenmode imperfection, Axisymmetric outward bulge and SPLA imperfection for ZKZ-XV50 model is presented in this section. Fig. 16 illustrates the comparison of the effect of imperfection amplitude on worst Eigenmode (n = 5), Axisymmetric outward bulge and SPLA – cone mid-section for axially compressed cylinder-cone-cylinder transition. From Fig. 16, it can be seen that at relatively small w_o/t, the axisymmetric outward bulge produces the greatest drop in the buckling strength of the cylinder-cone-cylinder assembly. However, as the w_o/t increases, the Eigenmode imperfection produces the worst knockdown factor. Overall, the obtained results indicated that Eigenmode imperfection gives the lowest reduction of buckling strength (i.e., knockdown factor) followed by Axisymmetric outward bulge and SPLA – cone mid-section. The

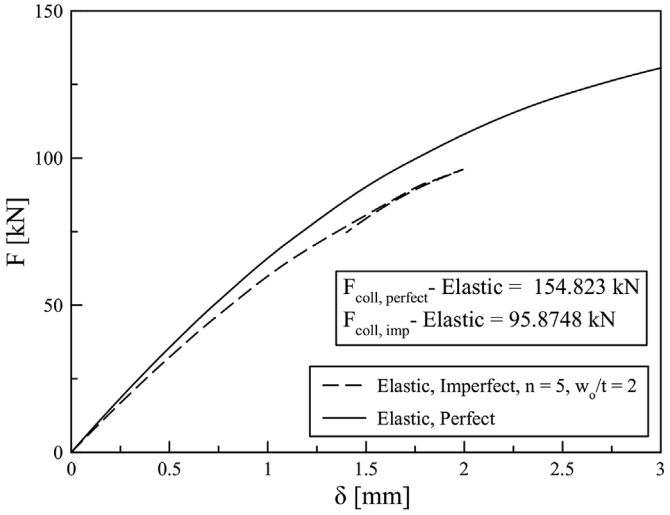

Fig. 10. Plot of perfect and imperfect load versus deflection curve of axially compressed cylinder-cone-cylinder intersections using elastic material modeling behavior.

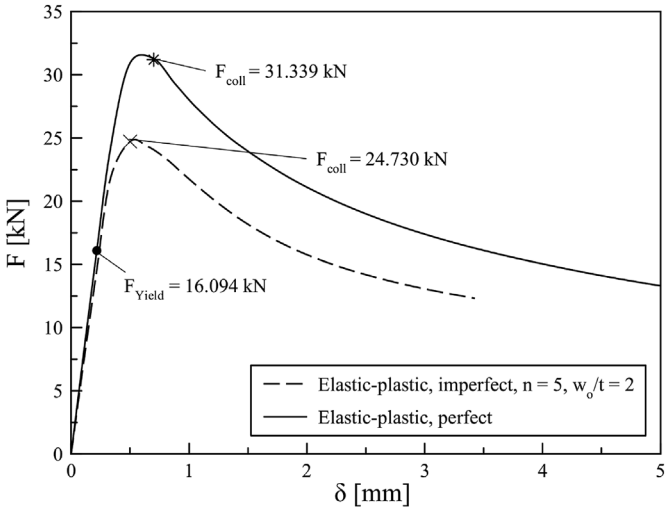

Fig. 11. Plot of perfect and imperfect load versus deflection curve of axially compressed cylinder-cone-cylinder intersections using elastic perfectly plastic material modeling behavior.

results indicated that Eigenmode imperfections approach are more conservative against the SPLA and Axisymmetric outward bulge imperfections curves. This finding is consistent with earlier work in the literature [15,23] for cylindrical shells. The knockdown factor predicted using the SPLA approach remains important for benchmarking purpose. Although, studies have shown that the use worst multiple perturbation load approach (WMPLA) may result in a much lower knock-down factor as compared to the dimple produced by a single perturbation load [32]. Moreover, from Ref. [30] models with 4 perturbation loads were seen to produce the worst result thereby producing the WMPLA. Hence, the use of WMPLA having 4 perturbation load at equidistance across the circumference on the cone mid-section was employed as an extension of the SPLA approach. It is assumed that the perturbation value is the same for all the 4 perturbation loads. The plot of knockdown factor from the WMPLA analysis is depicted in Fig. 16. From the analysis of this results it becomes clear that the WMPLA gives more conservation knock-down factor than the SPLA but less conservative than the eigenmode imperfection.

To widen the range of applicability of knockdown factor presented in this paper for practical application, numerical analysis was carried

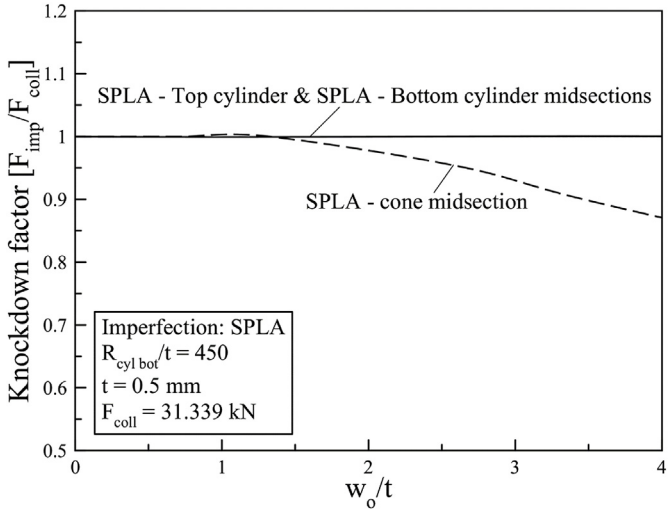

Fig. 12. Effect of imperfection amplitude and SPLA on the buckling strength of the cylinder-cone-cylinder transition.

out for cylinder-cone-cylinder assembly having different cone angles, i.e., 10°, 20° and 30° for the worst imperfection case in Fig. 16, i.e., eigenmode imperfection. The effect of imperfection amplitude on the load carrying capacity of cylinder-cone-cylinder assembly with different cone angles using Riks method, is shown in Fig. 17. From Fig. 17, it is apparent that cylinder-cone-cylinder transition with cone angle of 10° produce the lowest knockdown factor as compared to the same structure having cone angle of 20° and 30°. Further analysis was carried out in order to obtain the lower bound knockdown factor for design purpose. To this end, it was decided to examine the influence of eigenmode imperfection (worst imperfection case) having imperfection amplitude-to-thickness ratio, $w_o/t = 3$, on the buckling behavior of cylinder-cone-cylinder transition with different cone radius-to-thickness ratio, r_{cone}/t, and different cone angles. Fig. 18 depicts the plot of knockdown factor against the several cone radius-to-thickness ratios, thereby presenting a lower bound knockdown factor for design recommendation purposes. Although, the Eigenmode imperfection are usually too conservative [41], it is believed that this will be practically useful in design purposes as a safe and conservative method. The lower bound knockdown factor curve presented in this paper for cylinder-cone-cylinder transition is similar to that presented in NASA SP-8007 [32] guideline for isotropic cylindrical shells which was published several years ago but still relevant in most of the aerospace industries for preliminary design, since all the aerospace regulation agencies adopted this procedure as a safe and conservation approach. In the case of NASA SP-8007 guideline, NASA carried out a huge investment for about 5 years in the 60s on a project called 'Shell Buckling Knockdown Factor' in order to develop a new guideline to calculate the knockdown factor of isotropic cylinder subjected to buckling.

5. Conclusion

The results of finding following the numerical investigation on imperfection sensitivity of axially compressed cylinder-cone-cylinder transition are presented in this paper. For the foregoing analysis, the following conclusion can be drawn: (i) the buckling strength of cylinder-cone-cylinder shells was strongly affected by initial geometric imperfection and the reduction in buckling strength was seen to be considerably dependent on the approach and location of imperfection, (ii) the Eigenmode imperfection is seen to produce more conservative knockdown factor, followed by Axisymmetric outward bulge and SPLA imperfections, (iii) introducing the SPLA at cone low bottom significantly reacts with the highest sensitivity on small imperfection amplitude, and (iv) buckling strength is not affected at all for dimples at

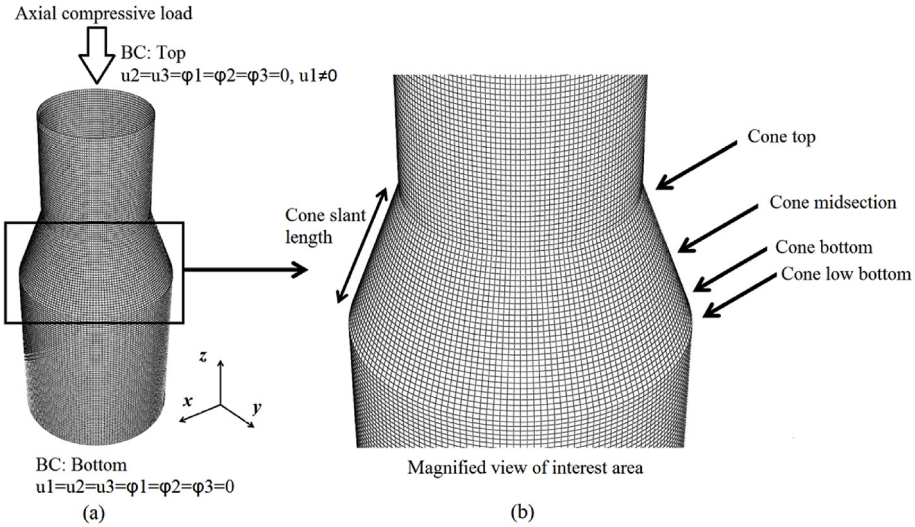

Fig. 13. (a) Full structure assembly with boundary condition and (b) location of applied lateral load along the cone slant length.

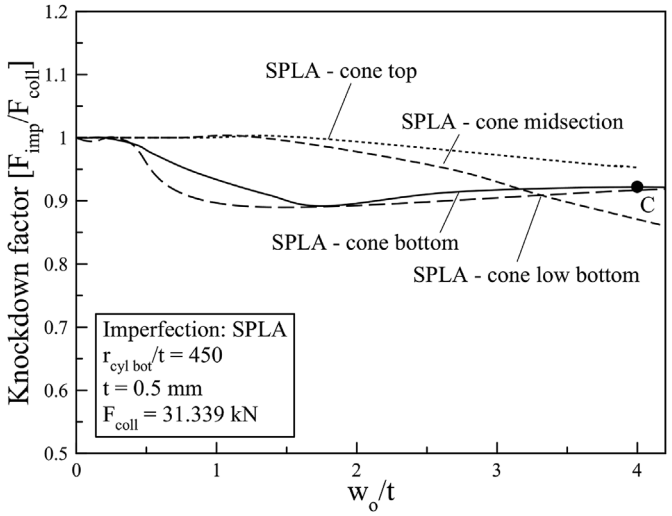

Fig. 14. Imperfection sensitivity of buckling load to the SPLA along the cone slant.

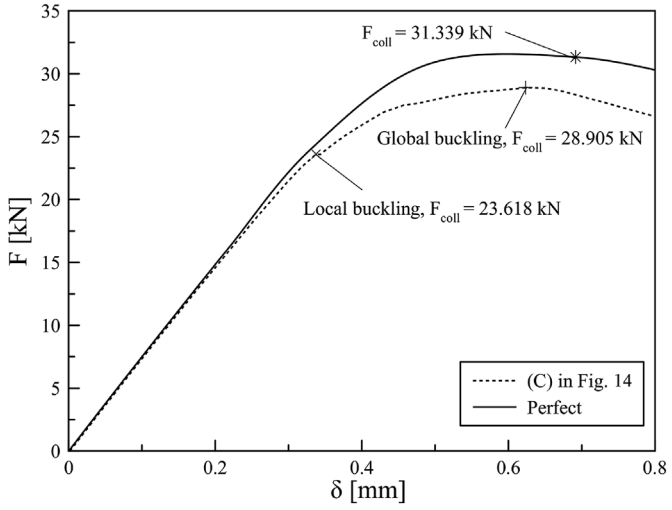

Fig. 15. Load-deflection curve for point (C) on Fig. 14 for cylinder-cone-cylinder transition with SPLA imperfection having imperfection amplitude, $w_o/t = 4$.

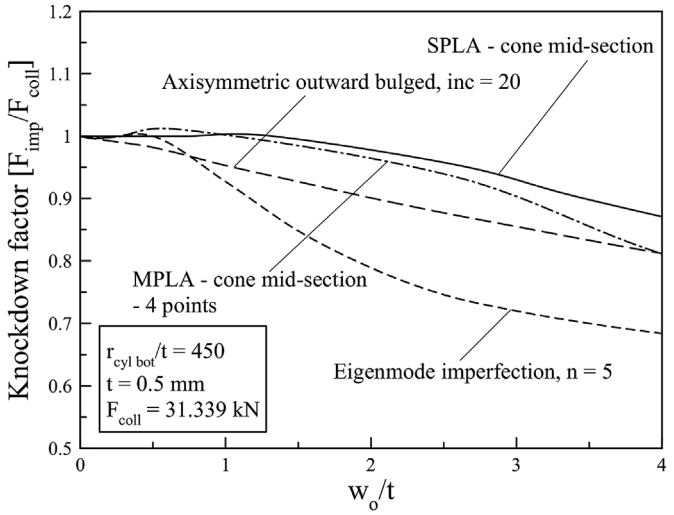

Fig. 16. Reduction of buckling strength as a function of imperfection amplitude, w_o/t. Comparison of imperfection amplitude between the worst Eigenmode imperfections, axisymmetric outward bulged, MPLA and SPLA curves.

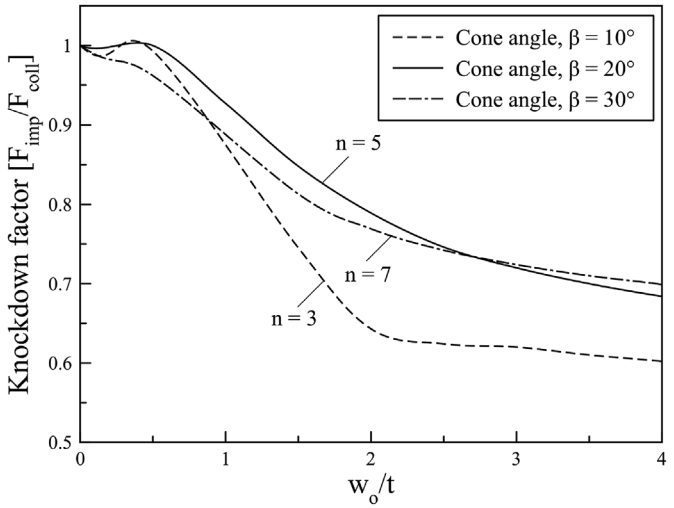

Fig. 17. Effect of imperfection amplitude and Eigenmode on the buckling strength of cylinder-cone-cylinder transition with different cone angles.

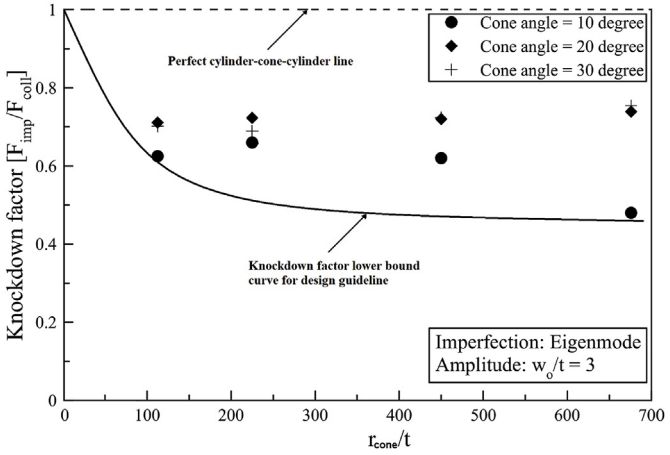

Fig. 18. Plot of worst imperfection (eigenmode) knockdown factor for cylinder-cone-cylinder transition having different cone radius-to-thickness ratio, r_{cone}/t.

both cylinder (i.e., top and bottom) midsections. To conclude, the lower bound knockdown factors curve that can be implemented for the design guideline for cylinder-cone-cylinder transition has been proposed for the worst imperfection case (Eigenmode imperfections).

Conflict of interest

The authors wish to declare that this is an original manuscript which has neither been previously nor simultaneously in whole or in part submitted anywhere else.

All the authors fairly have equal contributions in the manuscript. We will be grateful if you may kindly consider the manuscript for publication in your journal.

Acknowledgement

The authors would like to express their gratitude to Mr Mahzan Johar from Universiti Teknologi Malaysia for his technical assistance during the simulations. Also, the authors will like to acknowledge the financial support received from the Universiti Teknikal Malaysia Melaka and the Ministry of Education Malaysia under Fundamental Research Grant Scheme FRGS/2018/FTKMP-CARE/F00386.

References

[1] A. Zingoni, Discontinuity effects at cone-cone axisymmetric shell junctions, Thin-Walled Struct. 40 (2002) 877–891.
[2] A. Zingoni, B. Mokhothu, N. Enoma, A theoretical formulation for the stress analysis of multi-segmented spherical shells for high-volume liquid containment, Eng. Struct. 87 (2015) 21–31, https://doi.org/10.1016/j.engstruct.2015.01.002.
[3] F.G. Flores, L.A. Godoy, Post-buckling of elastic cone-cylinder and sphere-cylinder complex shells, Int. J. Press. Vessel. Pip. 45 (1991) 237–258, https://doi.org/10.1016/0308-0161(91)90095-J.
[4] J.G. Teng, Elastic buckling of cone-cylinder intersection under localized circumferential compression, Eng. Struct. 18 (1996) 41–48, https://doi.org/10.1016/0141-0296(95)00114-3.
[5] Y. Zhao, J.G. Teng, A stability design proposal for cone-cylinder intersections under internal pressure, Int. J. Press. Vessel. Pip. 80 (2003) 297–309, https://doi.org/10.1016/S0308-0161(03)00048-6.
[6] O. Ifayefunmi, J. Błachut, Imperfection Sensitivity: a review of buckling behaviour of cones, cylinders and domes, J. Press. Vessel Technol. (2018), https://doi.org/10.1115/1.4039695.
[7] J. Błachut, Experimental perspective on the buckling of pressure vessel components, Appl. Mech. Rev. 66 (2014) 1–24, https://doi.org/10.1115/1.4026067.
[8] A.C. Orifici, C. Bisagni, Perturbation-based Imperfection Analysis for Composite Cylindrical Shells Buckling in Compression, (2013).
[9] M.K. Chryssanthopoulos, C. Poggi, A. Spagnoli, Buckling design of conical shells based on validated numerical models, Thin-Walled Struct. 31 (1998) 257–270, https://doi.org/10.1016/S0263-8231(98)00006-8.
[10] M. Jabareen, I. Sheinman, Postbuckling Analysis of Geometrically Imperfect Conical Shells 132 (2007) 1326–1334, https://doi.org/10.1061/(ASCE)0733-9399(2006)132:12(1326).
[11] J. Zielnica, Imperfection sensitivity and stability of an elastic-plastic conical shell under axisymmetrical load, Arch. Appl. Mech. 72 (2002) 395–417, https://doi.org/10.1007/s00419-002-0216-y.
[12] J. Błachut, Interactive plastic buckling of cones subjected to axial compression and external pressure, Ocean Eng. 48 (2012) 10–16, https://doi.org/10.1016/j.oceaneng.2012.03.018.
[13] O. Ifayefunmi, J. Błachut, The effect of shape, thickness and boundary imperfections on plastic buckling of cones, Proc. ASME 2011 30th Int. Conf. Ocean. Offshore Arct. Eng. OMAE2011, 2011, pp. 1–11.
[14] O. Ifayefunmi, J. Błachut, Instabilities in imperfect thick cones subjected to axial compression and external pressure, Mar. Struct. 33 (2013) 297–307, https://doi.org/10.1016/j.marstruc.2013.06.004.
[15] M.S. Ismail, J. Purbolaksono, A. Andriyana, C.J. Tan, N. Muhammad, H.L. Liew, The use of initial imperfection approach in design process and buckling failure evaluation of axially compressed composite cylindrical shells, Eng. Fail. Anal. 51 (2015) 20–28, https://doi.org/10.1016/j.engfailanal.2015.02.017.
[16] S.G.P. Castro, R. Zimmermann, M.A. Arbelo, R. Khakimova, M.W. Hilburger, R. Degenhardt, Geometric imperfections and lower-bound methods used to calculate knock-down factors for axially compressed composite cylindrical shells, Thin-Walled Struct. 74 (2014) 118–132.
[17] S.G.P. Castro, R. Zimmermann, M.A. Arbelo, R. Degenhardt, Exploring the constancy of the global buckling load after a critical geometric imperfection level in thin-walled cylindrical shells for less conservative knock-down factors, Thin-Walled Struct. 72 (2013) 76–87, https://doi.org/10.1016/j.tws.2013.06.016.
[18] E. Eglitis, K. Kalnins, O. Ozolinsh, The influence of loading eccentricity on the buckling of axially compressed imperfect composite cylinders, Mech. Compos. Mater. 46 (2010) 483–492, https://doi.org/10.1007/s11029-010-9165-7.
[19] C. Bisagni, Dynamic buckling of fiber composite shells under impulsive axial compression, Thin-Walled Struct. 43 (2005) 499–514, https://doi.org/10.1016/j.tws.2004.07.012.
[20] J. Błachut, Combined stability of geometrically imperfect conical shells, Thin-Walled Struct. 67 (2013) 121–128.
[21] J. Błachut, Buckling of truncated cones with localized imperfections, Proc. ASME 2012 Press. Vessel. Pip. Conf. 2012, pp. 1–9.
[22] C. Hühne, R. Rolfes, E. Breitbach, J. Teßmer, Robust design of composite cylindrical shells under axial compression — simulation and validation, Thin-Walled Struct. 46 (2008) 947–962 http://linkinghub.elsevier.com/retrieve/pii/S0263823108000438, Accessed date: 7 July 2014.
[23] S.G.P. Castro, R. Zimmermann, M.A. Arbelo, R. Degenhardt, The single perturbation load approach compared with linear buckling mode-shaped , geometric dimple and measured imperfections for the buckling of cylindrical shells, Thin-Walled Struct. (2013) 1–14.
[24] H.N.R. Wagner, C. Hühne, R. Khakimova, Towards robust knockdown factors for the design of conical shells under axial compression, Int. J. Mech. Sci. 146–147 (2018) 60–80, https://doi.org/10.1016/j.ijmecsci.2018.07.016.
[25] R. Khakimova, C.J. Warren, R. Zimmermann, S.G.P. Castro, M. a. Arbelo, R. Degenhardt, The single perturbation load approach applied to imperfection sensitive conical composite structures, Thin-Walled Struct. 84 (2014) 369–377, https://doi.org/10.1016/j.tws.2014.07.005.
[26] M.A. Arbelo, R. Zimmermann, S.G.P. Castro, Comparison of new design guidelines for composite, Ninth Int. Conf. Compos. Sci. Technol., Sorrento, Italy, 2013, pp. 96–111.
[27] H.N.R. Wagner, C. Hühne, S. Niemann, R. Khakimova, Robust design criterion for axially loaded cylindrical shells - simulation and Validation, Thin-Walled Struct. 115 (2017) 154–162, https://doi.org/10.1016/j.tws.2016.12.017.
[28] R. Khakimova, S.G.P. Castro, D. Wilckens, K. Rohwer, R. Degenhardt, Buckling of axially compressed CFRP cylinders with and without additional lateral load: experimental and numerical investigation, Thin-Walled Struct. 119 (2017) 178–189, https://doi.org/10.1016/j.tws.2017.06.002.
[29] W.T. Haynie, M.W. Hilburger, Comparison of methods to predict lower bound buckling loads of cylinders under axial compression, 51st AIAA/ASME/ASCE/AHS/ASC, Struct. Struct. Dyn. Mater. Conf. (2010).
[30] M.A. Arbelo, R. Degenhardt, S.G.P. Castro, R. Zimmermann, Numerical characterization of imperfection sensitive composite structures, Compos. Struct. 108 (2014) 295–303, https://doi.org/10.1016/j.compstruct.2013.09.041.
[31] P. Hao, B. Wang, G. Li, Z. Meng, K. Tian, D. Zeng, X. Tang, Worst Multiple Perturbation Load Approach of stiffened shells with and without cutouts for improved knockdown factors, Thin-Walled Struct. 82 (2014) 321–330, https://doi.org/10.1016/j.tws.2014.05.004.
[32] V.I. Weingarten, P. Seide, J.P. Peterson, Buckling of Thin-Walled Circular Cylinders, NASA SP-8007 Monogr, (1968).
[33] H.N.R. Wagner, C. Hühne, K. Rohwer, S. Niemann, M. Wiedemann, Stimulating the realistic worst case buckling scenario of axially compressed unstiffened cylindrical composite shells, Compos. Struct. 160 (2017) 1095–1104, https://doi.org/10.1016/j.compstruct.2016.10.108.
[34] D. Dinkler, O. Knoke, Elasto-plastic limit loads of cylinder-cone configurations, J. Theor. Appl. Mech. 41 (2003) 443–457.
[35] ECCS, ECCS Publication - Buckling of Steel Shells: European Recommendations, (1988).
[36] E. Ore, D. Durban, Elastoplastic buckling of axially compressed circular cylindrical shells, Int. J. Mech. Sci. 34 (1992) 727–742.
[37] E. Ore, D. Durban, Elastoplastic buckling of annular plates in pure shear, ASME J. Appl. Mech 56 (1989) 644–651.
[38] J. Błachut, O. Ifayefunmi, Buckling of unstiffened steel cones subjected to axial compression and external pressure, Proceedings of the International Conference on Ocean, Offshore and Arctic Engineering (OMAE, vol. 2, ASME, NY, USA, 978-0-

7918-4910-1, 2010, pp. 385–398 OMAE2010-20518.
[39] J. Błachut, O. Ifayefunmi, M A. Corfa, Collapse and buckling of conical shells, Proceedings of the International Offshore (Ocean) and Polar Engineering Conference, ISOPE-2011 TPC-296, pp. 887-893, Cupertino, California, USA (ISBN 978-1-880653-96-8).
[40] J. Błachut, Buckling of composite domes with localised imperfections and subjected to external pressure, Compos. Struct. 153 (2016) 746–754, https://doi.org/10.1016/j.compstruct.2016.07.007.
[41] P. Hao, B. Wang, K. Tian, K. Du, X. Zhang, Influence of imperfection distributions for cylindrical stiffened shells with weld lands, Thin-Walled Struct. 93 (2015) 177–187.